

# Nuclear level densities and $\gamma$ -ray strength functions of $^{180,181}\text{Ta}$ and neutron capture cross sections

K.L. Malatji<sup>1,2,3,a</sup>, B.V. Kheswa<sup>1,4,b</sup>, M. Wiedeking<sup>1,c</sup>, F.L. Bello Garrote<sup>4</sup>, C.P. Brits<sup>1,3</sup>, D.L. Bleuel<sup>5</sup>, F. Giacoppo<sup>6,7</sup>, A. G6rgen<sup>4</sup>, M. Guttormsen<sup>4</sup>, K. Hadynska-Klek<sup>4</sup>, T.W. Hagen<sup>4</sup>, V.W. Ingeberg<sup>4</sup>, M. Klintefjord<sup>4</sup>, A.C. Larsen<sup>4</sup>, H.T. Nyhus<sup>4</sup>, T. Renstr6m<sup>4</sup>, S. Rose<sup>4</sup>, E. Sahin<sup>4</sup>, S. Siem<sup>4</sup>, G.M. Tveten<sup>4</sup>, and F. Zeiser<sup>4</sup>

<sup>1</sup> iThemba LABS, PO Box 722, Somerset West, 7129, South Africa

<sup>2</sup> Physics Department, University of the Western Cape, Bellville 7535, South Africa

<sup>3</sup> Physics Department, University of Stellenbosch, Matieland 7602, South Africa

<sup>4</sup> Department of Physics, University of Oslo, 0316 Oslo, Norway

<sup>5</sup> Lawrence Livermore National Laboratory, 7000 East Avenue, Livermore, CA 94550-9234, USA

<sup>6</sup> Helmholtz Institute Mainz, 55099 Mainz, Germany

<sup>7</sup> GSI Helmholtzzentrum f6ur Schwerionenforschung, 64291 Darmstadt, Germany

**Abstract.** The  $\gamma$ -ray strength functions and nuclear level densities in the quasi-continuum of  $^{180,181}\text{Ta}$  are extracted from particle- $\gamma$  coincidence events with the Oslo Method, below the  $S_n$ . The data were used as input in the TALYS reaction code for calculations of the astrophysical Maxwellian-averaged ( $n, \gamma$ ) cross-sections to investigate nucleosynthesis of nature's rarest stable isotope  $^{180}\text{Ta}$ .

## 1. Introduction

A small number of naturally occurring neutron-deficient nuclides with  $Z \geq 34$  referred to as  $p$ -nuclei cannot be produced by stellar neutron-capture processes, while almost all  $p$ -nuclei with  $A > 110$  are thought to be produced by the photodisintegration of  $s$ - and  $r$ -process seed nuclei. However, for some nuclear systems, these processes are not sufficient to explain their observed solar abundance and their origin is still not well understood. Calculations of the  $^{180}\text{Ta}$  production in the universe are often controversial since several processes, sometimes exclusively, could reproduce the observed  $^{180}\text{Ta}$  abundance in the cosmos, making it a particularly interesting case to study. A peculiar feature of  $^{180}\text{Ta}$  is that it is the rarest isotope in the solar system, which exists in a  $9^-$  isomeric state at  $E_x = 77$  keV ( $t_{1/2,iso} > 10^{15}$  yr), with an isotopic abundance of about 0.012%. Over the years many processes, such as slow and rapid neutron capture reactions ( $s$ -process,  $r$ -process) in stars and supernova explosions, photon- and neutrino-induced reactions in supernovae, have been proposed to be the production mechanism of  $^{180}\text{Ta}$ . However, no consensus exists and it has been theoretically shown that  $^{180}\text{Ta}$  could be exclusively explained with the ( $\gamma, n$ )  $p$ -process reaction [1]. The  $s$ -process can explain the production of  $^{180}\text{Ta}$ , as well, mostly via branching in  $^{179}\text{Hf}$  through the reaction  $^{179}\text{Hf}(\beta^-)^{179}\text{Ta}(n, \gamma)^{180}\text{Ta}$  and/or  $^{179}\text{Hf}(n, \gamma)^{180m}\text{Hf}(\beta^-)^{180}\text{Ta}$  [2].

Furthermore, more exotic reactions such as neutrino ( $\nu$ ) processes, which include  $^{180}\text{Hf}(\nu_e, e)^{180}\text{Ta}$  and  $^{181}\text{Ta}(\nu, \nu' n)^{180}\text{Ta}$ , have been proposed to partly explain

its synthesis [3–5]. Since the astrophysical sites for the nucleosynthesis of  $^{180}\text{Ta}$  remain unknown, a combination of the above processes is undeniably possible. However, the significance of individual processes cannot be clearly determined, as a result of the uncertainties on the reaction rates for  $^{180}\text{Ta}$  due to unavailability of experimental data, such as the nuclear level density (NLD) and  $\gamma$ -ray strength function ( $\gamma\text{SF}$ ) [6]. The NLD is described as the average number of nuclear energy levels as a function of excitation energy  $E_x$ , while the  $\gamma\text{SF}$  gives a measure of the average transition probability for a  $\gamma$ -ray decay. Both nuclear properties are critical for the Hauser-Feshbach formalism, which is implemented in the statistical nuclear reaction code TALYS [7], which is used here to calculate astrophysical neutron capture reaction rates of  $^{179,180m}\text{Ta}$ .

In the present case study, the  $^{180,181}\text{Ta}$   $\gamma\text{SF}$  and NLD below the neutron separation energy,  $S_n$ , were investigated using the Oslo Method [8]. These results are used to determine the corresponding astrophysical Maxwellian-averaged ( $n, \gamma$ ) cross-sections (MACS) which in turn will be utilized in astrophysical network calculations to investigate nucleosynthesis of  $^{180}\text{Ta}$ . In Sect. 2, we present experimental details and an overview of the data analysis. In Sect. 3, we discuss the results and use our data to estimate MACS for the  $^{179}\text{Ta}(n, \gamma)^{180gs}\text{Ta}$  and  $^{180m}\text{Ta}(n, \gamma)^{181}\text{Ta}$  reactions, and their implications for the  $^{180}\text{Ta}$  nucleosynthesis.

## 2. Experimental analysis and results

The particle- $\gamma$  coincidence experiment was performed at the Oslo Cyclotron Laboratory (OCL) using 34 MeV  $^3\text{He}$  beam, with an average intensity of  $\approx 2$  nA, to populate excited states in  $^{180,181}\text{Ta}$  through the ( $^3\text{He}, ^3\text{He}'\gamma$ ) and

<sup>a</sup> e-mail: kgashanel@gmail.com

<sup>b</sup> e-mail: bngkheswa@gmail.com

<sup>c</sup> e-mail: wiedeking@tlabs.ac.za

( $^3\text{He}, \alpha\gamma$ ) reactions. A  $0.8 \text{ mg/cm}^2$  thick self-supporting  $^{181}\text{Ta}$  foil was used as a target. The charged ejectiles in coincidence with  $\gamma$ -rays were recorded with eight  $\Delta E - E$  silicon ring particle telescope array (SiRi) [9] and the  $\gamma$ -rays were recorded using the high-efficiency multi-detector NaI(Tl) array (CACTUS) [10].

The SiRi array was mounted inside the target chamber 5 cm away from the target and placed at backward angles, covering an mean scattering angular range of  $\theta \approx 126^\circ$  to  $140^\circ$  in steps of  $2^\circ$ , with respect to the beam axis. The 8-fold segmented front ( $\Delta E$ ) and back ( $E$ ) detectors have thicknesses of  $\approx 130 \mu\text{m}$  and  $1550 \mu\text{m}$ , respectively, giving a total of 64  $\Delta E - E$  particle telescopes. A  $10.5 \mu\text{m}$  thick aluminium foil was placed in front of the  $\Delta E - E$  telescopes, to shield  $\delta$ -electrons. The average energy resolution<sup>1</sup> of the SiRi array is  $\approx 350 \text{ keV}$ , for ( $^3\text{He}, ^3\text{He}'\gamma$ ) $^{181}\text{Ta}$  reaction. The CACTUS array consists of 26 collimated cylindrical NaI(Tl) detectors with crystal dimensions of  $5'' \times 5''$  each. The crystals are surrounded by a 3 mm thick lead shield to reduce crosstalk between neighboring detectors and are positioned 22 cm away from the target. The CACTUS array has a total efficiency and resolution of 14.1% and 7% FWHM for a 1332 keV  $\gamma$ -ray transition, respectively. A valid trigger for the analog-to-digital converters (ADCs) is constructed when a  $\Delta E - E$  Si event is in coincidence with a NaI(Tl) event within the ADC master gate. The measured  $^3\text{He}$  and  $\alpha$  energies were transformed to  $E_x$  of residual nuclei  $^{181}\text{Ta}$  and  $^{180}\text{Ta}$ , using reaction kinematics, different Q-values and energy losses. As a result, the respective  $E_x$  versus  $\gamma$ -ray energy,  $E_\gamma$ , matrices can then be extracted from the particle- $\gamma$  coincidence events spectra.

The  $\gamma$ -ray spectra, extracted for each  $E_x$  bin, were unfolded using unfolding iterative procedure and then corrected for the known response functions of the CACTUS array [11], to obtain the full-energy  $\gamma$ -ray spectra. At this point, the first-generation method [12] is used to extract the primary  $\gamma$ -rays, from the  $\gamma$  rays that emerge from later steps in the decay cascades at each  $E_x$  bin of the continuum  $\gamma$ -ray spectra. The resulting experimental first generation matrix, which is a distribution of primary  $\gamma$ -rays as a function of  $E_\gamma$  and  $E_x$ ,  $P(E_x, E_\gamma)$ , is shown in Fig. 1. The two regions that correspond to  $E_\gamma = 400$  and  $1300 \text{ keV}$  are dominated by low statistics due to over-subtraction of discrete and strong  $\gamma$ -ray transitions during the generation of primary  $\gamma$ -ray matrix. Both nuclei under study had low statistics.

The NLD and  $\gamma$ SF of  $^{180,181}\text{Ta}$  were extracted simultaneously from  $P(E_x, E_\gamma)$  through an iterative procedure [8], using the ansatz:

$$P(E_x, E_\gamma) \propto \rho(E_f)\mathcal{T}(E_\gamma) \quad (1)$$

where the decay probability,  $P(E_x, E_\gamma)$ , of a  $\gamma$ -ray with energy  $E_\gamma$  to be emitted from a specific initial excited state, with energy  $E_x$ , is proportional to the NLD  $\rho(E_f)$  of the final state, with energy  $E_f = E_x - E_\gamma$ , and the  $\gamma$ -ray transmission coefficient  $\mathcal{T}(E_\gamma)$ . The relationship in Eq. (1) is only appropriate at high NLDs, assuming that the Brink Hypothesis [13] holds for all types of collective decay modes and that the transition

<sup>1</sup> The energy resolution of the particle telescope is determined by measuring the full width half maximum (FWHM) of the  $^3\text{He}$  beam elastically scattering off the  $^{181}\text{Ta}$  target.

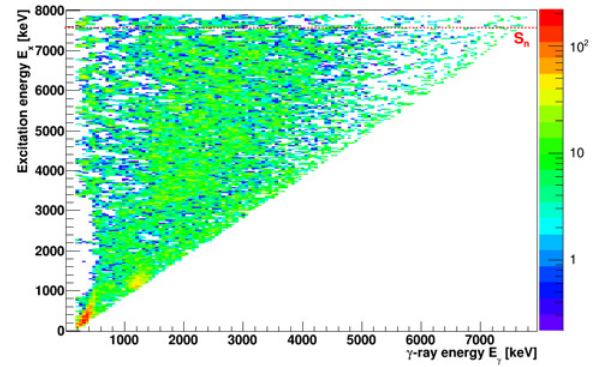


**Figure 1.** The experimental first generation matrix for  $^{181}\text{Ta}$ .

**Table 1.** Parameters used for normalization of  $\rho(E_x)$  and  $\mathcal{T}(E_\gamma)$  in  $^{180,181}\text{Ta}$ , where  $\sigma$  is the spin cut-off parameter at ( $S_n$ ).

Isotope	$\sigma$	$D_0$ (eV)	$\rho(S_n)$ ( $10^6 \text{ MeV}^{-1}$ )	$\langle \Gamma_\gamma(S_n) \rangle$ (meV)
$^{180}\text{Ta}$	$4.93 \pm 0.49^a$	$0.80 \pm 0.23^b$	$10.67 \pm 3.50^b$	$62.0 \pm 5.77^b$
$^{181}\text{Ta}$	$4.96 \pm 0.50^a$	$1.11 \pm 0.11^c$	$14.58 \pm 2.76^a$	$51.0 \pm 1.58^c$

<sup>a</sup>Calculated with the back-shifted Fermi gas model [19].

<sup>b</sup>Estimated values.

<sup>c</sup>Average value from Refs. [20,21].

probability for a decay into any specific combination of final states is independent of how the compound nucleus [14] was formed. Henceforth,  $\rho(E_f)$  and  $\mathcal{T}(E_\gamma)$  can be extracted using an iterative procedure [8], where the theoretical first-generation  $\gamma$ -ray matrices  $P_{th}(E_x, E_\gamma)$  are fitted to the experimental first-generation  $\gamma$ -ray matrices  $P(E_x, E_\gamma)$  by performing a global  $\chi^2$  minimization. A global  $\chi^2$  minimum was achieved in the energy regions of  $E_\gamma > 1634 \text{ keV}$  and  $2569 \text{ keV} \leq E_x \leq 7376 \text{ keV}$  for  $^{181}\text{Ta}$ , and  $E_\gamma > 1734 \text{ keV}$  and  $2969 \text{ keV} \leq E_x \leq 6348 \text{ keV}$  for  $^{180}\text{Ta}$ .

Once the  $\rho(E_f)$  and  $\mathcal{T}(E_\gamma)$  have been simultaneously extracted, there exist infinitely many solutions, for the  $\chi^2$  above, of the form:

$$\tilde{\rho}(E_f) = A\rho(E_f)e^{\alpha E_f} \quad (2)$$

and

$$\tilde{\mathcal{T}}(E_\gamma) = B\mathcal{T}(E_\gamma)e^{\alpha E_\gamma} \quad (3)$$

where  $\alpha$ ,  $A$  and  $B$  are the normalization parameters, which correspond to physical solutions. The parameters  $\alpha$  and  $A$  are determined by normalizing  $\tilde{\rho}$  to the level density of known discrete states at low  $E_x$  and to  $\rho(S_n)$  (calculated from experimental average neutron resonance spacing,  $D_0$ ) at high  $E_x$ , and  $B$  is calculated from the average total radiative width  $\langle \Gamma_\gamma(S_n) \rangle$ . In the case of  $^{180}\text{Ta}$ , neither  $D_0$  nor  $\langle \Gamma_\gamma(S_n) \rangle$  are known in the literature, since the target nuclei for ( $n, \gamma$ ) reactions is unstable. Therefore, using the spline fit, as implemented in TALYS [7],  $\langle \Gamma_\gamma(S_n) \rangle$  was estimated. The  $\rho(S_n)$  was estimated by normalizing both  $\rho(E_x)$  and  $\mathcal{T}(E_\gamma)$  of  $^{180}\text{Ta}$  on the basis of having the same slope as  $\rho(E_x)$  and  $\mathcal{T}(E_\gamma)$  of  $^{181}\text{Ta}$ . It has been shown that  $\rho(E_x)$  and  $\mathcal{T}(E_\gamma)$  of neighboring isotopes have the same slope [15–17]. The value of  $\rho(S_n)$  was then used to calculate  $D_0$  of  $^{180}\text{Ta}$  using equation (20) of Ref. [18]. The NLD of  $^{180,181}\text{Ta}$  are shown in Fig. 2.

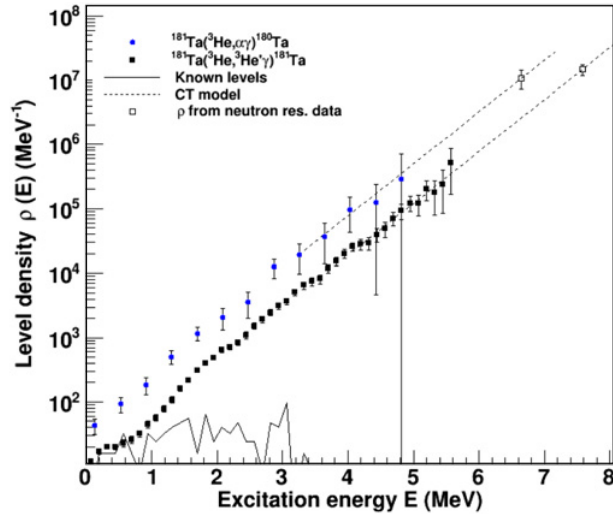


**Figure 2.** The extracted NLDs of  $^{180,181}\text{Ta}$ . The  $^{181}\text{Ta}$  data points are normalized to known discrete levels (solid line) at low  $E_x$  and to the level density at the  $S_n$  (open square) using an interpolation with the Constant Temperature model [22] (dashed line).

Assuming dipole transitions, the experimental  $\gamma$ SF,  $f(E_\gamma)$ , is related to  $\gamma$ -ray transmission coefficient by

$$f(E_\gamma) = \frac{BT(E_\gamma)}{2\pi E_\gamma^3}. \quad (4)$$

The extracted  $^{181}\text{Ta}$   $\gamma$ SF is compared to various known data as shown in Fig. 3. The two components of the giant electric dipole resonance, (GEDR) are fitted with enhanced generalized Lorentzian functions (EGLO) [25],  $f_{GEDR1}(E_\gamma)$  and  $f_{GEDR2}(E_\gamma)$ , at  $E_\gamma \approx 12.6\text{ MeV}$  and  $15.9\text{ MeV}$ . A constant nuclear temperature of  $T_f = 0.47\text{ MeV}$ , which was treated as a free parameter, was considered for the temperature dependence width  $\langle\Gamma_\gamma\rangle$ . This is consistent with the Brink hypothesis assumed in the Oslo method, since  $T_f$  is constant with increasing  $E_x$ . In addition to the GEDR, a weaker resonance was also fitted using the Standard Lorentzian functions (SLO),  $f_{Res2}(E_\gamma)$  at  $E_\gamma \approx 6.7\text{ MeV}$ . This resonance was recently observed [26] and was considered as E1 pygmy resonance. The SLO  $f_{Res1}(E_\gamma)$  was used to fit the additional strength at  $E_\gamma \approx 4.8\text{ MeV}$ , although the electromagnetic character is unknown, and  $f_{Res3}(E_\gamma)$  to fit the M1 spin-flip resonance at  $E_\gamma \approx 7.5\text{ MeV}$ . Therefore, the total model prediction of the  $\gamma$ SF is given by  $f_{total}(E_\gamma) = f_{Res1}(E_\gamma) + f_{Res2}(E_\gamma) + f_{Res3}(E_\gamma) + f_{GEDR1}(E_\gamma) + f_{GEDR2}(E_\gamma)$ . The fitted functions clearly reproduce the  $(\gamma,x)$  data together with the measured low-energy data.

### 3. Discussion and future outlook

The  $^{180,181}\text{Ta}$   $\gamma$ SFs show no pronounced features, except for the observed enhancement in the strength function from 6 MeV termed ‘‘Res2’’ resonance in  $^{181}\text{Ta}$  which may be related to E1 pygmy resonance (see Fig. 3). Besides the E1 pygmy resonance, the  $^{181}\text{Ta}$   $\gamma$ SF is relatively featureless with only a weak resonance at  $E_\gamma \approx 4.8\text{ MeV}$ , and certainly no low-energy enhancement. The NLD for odd-odd  $^{180}\text{Ta}$  is higher than that of the even-odd  $^{181}\text{Ta}$  (see Fig. 2). This is expected, due to one extra unpaired neutron

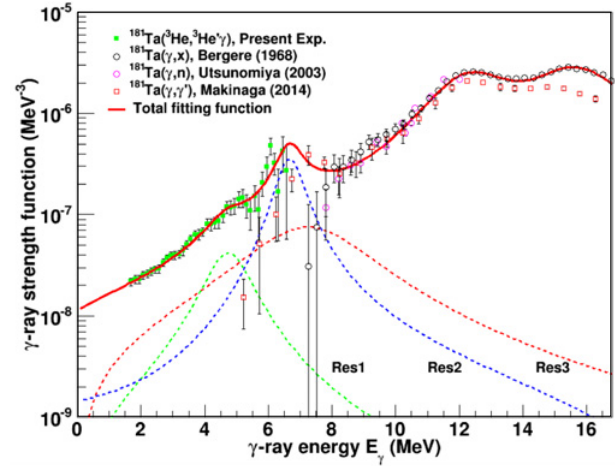


**Figure 3.** Comparison of data obtained from  $^{181}\text{Ta}(\gamma,n)$  [23] and  $^{181}\text{Ta}(\gamma,xn)$  photo-neutron reactions [24] with experimental  $\gamma$ SF of  $^{181}\text{Ta}$ . Res1, 2 and 3 represent extra strengths fitted with the Standard Lorentzian functions [25].

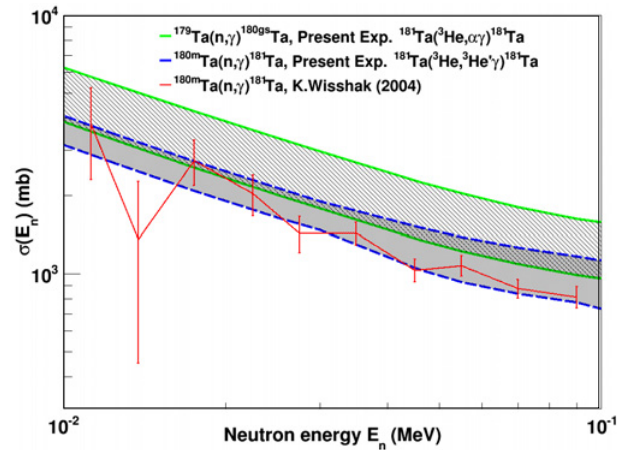


**Figure 4.** The present  $^{180m}\text{Ta}(n,\gamma)^{181}\text{Ta}$  (blue line) and  $^{179}\text{Ta}(n,\gamma)^{180g5}\text{Ta}$  (green line) neutron capture cross sections as a function of neutron energy, together with the previously measured  $^{180m}\text{Ta}(n,\gamma)^{181}\text{Ta}$  cross sections [28].

in  $^{180}\text{Ta}$  which increases the number of degrees of freedom. In the region around 2 MeV of the  $^{181}\text{Ta}$  NLD, a small change in the slope is observed which can be explained as Cooper pair breaking.

Assuming the principle of detailed balance to be valid [27], the  $(n,\gamma)$  cross sections and the reverse photo-neutron emission rates of astrophysical relevance, as well as the MACS, were estimated for both  $^{180,181}\text{Ta}$  isotopes. The calculations were achieved using the statistical nuclear reactions code TALYS (version 1.6). Figure 4 shows the final  $(n,\gamma)$  cross sections,  $\sigma(E_n)$ , as a function of incident neutron energies,  $E_n$ , taking into account the uncertainties affecting the  $\gamma$ SFs and the NLDs. The  $(n,\gamma)$  cross sections of  $^{180m}\text{Ta}$  from Ref. [28] are shown for comparison. Our  $^{180m}\text{Ta}(n,\gamma)$  cross sections show good agreement with the previously measured  $^{180m}\text{Ta}(n,\gamma)$  cross sections [28], within the error bars.

The astrophysical MACS were calculated for both  $^{179,180m}\text{Ta}(n,\gamma)$  reactions, at the  $s$ - and  $p$ -process thermal energies of  $kT = 30\text{ keV}$  and  $kT = 215\text{ keV}$ , respectively, using the newly determined NLDs and  $\gamma$ SFs. At  $kT = 215\text{ keV}$ , the  $^{179,180m}\text{Ta}(n,\gamma)$  reaction rates amount to

$\langle\sigma_v\rangle = 793_{-186}^{+241}$  mb and  $574_{-53}^{+49}$  mb, respectively. It can be noted that the  $^{181}\text{Ta}(\gamma, n)$  reaction rates are about 28% less than the destructive  $^{180g^s}\text{Ta}(\gamma, n)$  reaction rates. At  $kT = 30$  keV, the  $^{179,180m}\text{Ta}(n, \gamma)$  reaction rates amount to  $\langle\sigma_v\rangle = 2445_{-349}^{+482}$  mb and  $2047_{-146}^{+129}$  mb, respectively. These newly calculated  $^{179,180m}\text{Ta}(n, \gamma)$   $\langle\sigma_v\rangle$  values are 45% and 28% larger than the MACS from KADoNiS [29], respectively. The possible  $s$ -process production of  $^{180}\text{Ta}$ , occurs mostly via beta-decay branching from an excited state in  $^{179}\text{Hf}$  according to Ref. [2]. To further investigate the  $s$ -process production of  $^{180}\text{Ta}$ , relevant cross sections of neighboring nuclei need to be experimentally investigated as well.

Future measurements of the NLD and  $\gamma\text{SF}$  are essential to obtain experimentally constrained  $(n, \gamma)$  cross sections to investigate galactic production mechanism of  $^{180}\text{Ta}$  from various processes and astrophysical sites.

NRF South Africa is acknowledged, for project Grant No. 92789 and the support from the IAEA under Research Contract 20454. A.C.L acknowledges funding from ERC-STG-2014 Grant Agreement No. 637686. G.M.T acknowledge funding from the Research Council of Norway, Project Grant No. 222287. Many thanks to J.C. Müller, A. Semchenkov, and J.C. Wikne for providing quality beam.

## References

- [1] M. Rayet et al., *A&A* **298**, 517 (1995)
- [2] S. Bisterzo et al., *MNRAS* **499**, 506–527 (2015)
- [3] S.E. Woosley et al., *Astrophys. J.* **356**, 272 (1990)
- [4] A. Heger et al., *Phys. Lett. B* **606**, 258 (2005)
- [5] A. Byelikov et al., *Phys. Rev. Lett.* **98**, 082501 (2007)
- [6] S. Goriely et al., *A&A J.* **375**, L35 (2001)
- [7] A.J. Koning et al., *Nuclear Data for Science and Technology* (EDP Sciences; eds O. Bersillon et al.), p. 211 (2008) (see also <http://www.talys.eu>)
- [8] A. Schiller et al., *Nucl. Instrum. Methods Phys. Res. A* **447**, 498 (2000)
- [9] M. Guttormsen et al., *Nucl. Instrum. Methods Phys. Res. A* **648**, (2011)
- [10] M. Guttormsen et al., *Phys. Scr.* **T32**, 54 (1990)
- [11] M. Guttormsen et al., *Nucl. Instrum. Methods Phys. Res. A* **374**, 371 (1996)
- [12] M. Guttormsen et al., *Nucl. Instrum. Methods Phys. Res. A* **255**, 518 (1987)
- [13] D.M. Brink, *Doctoral Thesis*, Oxford University, 1955, pp. 101–110
- [14] A. Bohr, B. Mottelson, *Nuclear Structure*, Vol. I (Benjamin, New York, 1969)
- [15] A.C. Larsen et al., *Phys. Rev. C* **87**, 014319 (2013)
- [16] H.T. Nyhus et al., *Phys. Rev. C* **85**, 014323 (2012)
- [17] S. Siem et al., *Phys. Rev. C* **65**, 044318 (2002)
- [18] A.C. Larsen et al., *Phys. Rev. C* **83**, 034315 (2011)
- [19] T. von Egidy, D. Bucurescu, *Phys. Rev. C* **80**, 054310 (2009)
- [20] R. Capote et al., *Reference Input Parameter Library, RIPL-2 and RIPL-3*; available online at <http://www-nds.iaea.org/RIPL-3/> (2009)
- [21] S.F. Mughabghab, *Atlas of Neutron Resonances*, (Elsevier Science, Amsterdam, 2006). 5<sup>th</sup> ed
- [22] A. Gilbert, A.G.W. Cameron, *Can. J. Phys.* **43**, 1446 (1965)
- [23] H. Utsunomiya et al., *Phys. Rev. C* **67**, 015807 (2003)
- [24] R. Bergere et al., *Nucl. Phys. A* **121**, 463 (1968)
- [25] J. Kopecky, M. Uhl, *Phys. Rev. C.* **41**, 1941 (1990)
- [26] A. Makinaga et al., *Phys. Rev. C* **90**, 044301 (2014)
- [27] J. Holmes, S. Woosley, W. Fowler, B. Zimmerman, *Atomic Data and Nuclear Data Tables* **18**, 305 (1976)
- [28] K. Wisshak et al., *Phys. Rev. C* **69**, 055801 (2004)
- [29] I. Dillmann et al., *AIP Conf. Proc.* 819, 123; online at <http://www.kadonis.org>